


ORIGINAL RESEARCH

Open Access



Test-retest reproducibility of [^{11}C]-L-deprenyl- D_2 binding to MAO-B in the human brain

Ryosuke Arakawa^{1*} , Per Stenkrona¹, Akihiro Takano¹, Sangram Nag¹, Rafael S. Maior^{1,2} and Christer Halldin¹

Abstract

Background: [^{11}C]-L-deprenyl- D_2 is a positron emission tomography (PET) radioligand for measurement of the monoamine oxidase B (MAO-B) activity in vivo brain. The estimation of the test-retest reproducibility is important for accurate interpretation of PET studies.

Results: We performed two [^{11}C]-L-deprenyl- D_2 scans for six healthy subjects and evaluated the test-retest variability of this radioligand. MAO-B binding was quantified by two tissue compartment model (2TCM) with three rate constants (K_1 , k_2 , k_3) using metabolite-corrected plasma radioactivity. The λk_3 defined as $(K_1/k_2) \times k_3$ was also calculated. The correlation between MAO-B binding and age, and the effect of partial volume effect correction (PVEc) for the reproducibility were also estimated. %difference of k_3 was 2.6% (medial frontal cortex) to 10.3% (hippocampus), and that of λk_3 was 5.0% (thalamus) to 9.2% (cerebellum). Mean %difference of all regions were 5.3 and 7.0% in k_3 and λk_3 , respectively. All regions showed below 10% variabilities except the hippocampus in k_3 (10.3%). Intraclass correlation coefficient (ICC) of k_3 was 0.78 (hippocampus) to 0.98 (medial frontal cortex), and that of λk_3 was 0.78 (hippocampus) to 0.95 (thalamus). Mean ICC were 0.94 and 0.89 in k_3 and λk_3 , respectively. The highest positive correlation with age was observed in the hippocampus, as $r = 0.75$ in k_3 and 0.76 in λk_3 . After PVEc, mean %difference were 5.6 and 7.2% in k_3 and λk_3 , respectively. Mean ICC were 0.92 and 0.90 for k_3 and λk_3 , respectively. These values were almost the same as those before PVEc.

Conclusions: The present results indicate that k_3 and λk_3 of [^{11}C]-L-deprenyl- D_2 are reliable parameters for test-retest reproducibility with healthy subjects both before and after PVEc. The studies with patients of larger sample size are required for further clinical applications.

Keywords: Age effect, [^{11}C]-L-deprenyl- D_2 , Monoamine oxidase B, Partial volume effect correction, Positron emission tomography, Test-retest variability

Background

Monoamine oxidase (MAO) is an enzyme of deamination of monoamine and exists in two isoforms, MAO-A and MAO-B. MAO-B is considered as a major enzyme in dopamine metabolism in the human brain, and MAO-B inhibitors are used for the treatment of Parkinson's disease to increase the dopamine level [1]. For Alzheimer's disease (AD), several studies reported the upregulation of MAO-B expression related to the neuroinflammatory

process in the glia cells [2–6]. So, inhibition of MAO-B is expected to have beneficial effects in AD by reducing neurodegenerative processes.

[^{11}C]-L-deprenyl- D_2 is a positron emission tomography (PET) radioligand for measurement of the MAO-B activity in the brain [7]. This radioligand was used for many PET studies to evaluate MAO-B inhibitors' occupancy [8, 9], pathology of AD [10–12], amyotrophic lateral sclerosis (ALS) [13], traumatic brain injury [14], and epilepsy [15–17]. In addition to the clinical studies, [^{11}C]-L-deprenyl- D_2 showed good result reproducibility in a test-retest protocol [18].

Recently, we reported the brain occupancy of MAO-B using [^{11}C]-L-deprenyl- D_2 after administration of a

* Correspondence: ryosuke.arakawa@ki.se

¹Department of Clinical Neuroscience, Center for Psychiatry Research, Karolinska Institutet and Stockholm County Council, Stockholm, Sweden
Full list of author information is available at the end of the article

MAO-B inhibitor, sebragiline, in controls and patients with AD [9]. Although the good reproducibility of [^{11}C]-L-deprenyl- D_2 has already been reported, confirmation in test-retest variability studies by using identical protocol settings, including radioligand production and PET machine, is helpful for accurate interpretation of occupancy. Additionally, age effect of [^{11}C]-L-deprenyl- D_2 should be estimated since an increase of MAO-B expression has been reported in elderly subjects by postmortem [19] and in vivo PET [20] studies. The partial volume effect (PVE) should be also considered in the PET studies for aged subjects or AD patients with brain atrophy [21, 22].

In this study, we focused on three issues. First, we evaluated the test-retest variability of [^{11}C]-L-deprenyl- D_2 in the healthy subjects who were scanned twice. Second, the correlation between MAO-B activity and age was estimated. Finally, the effect of partial volume effect correction (PVEc) for the reproducibility was also estimated.

Methods

Subjects

Six healthy volunteers (age range, 21–62 years; mean \pm SD, 39.0 ± 17.0 ; four males, two females) were enrolled in the study. None had a history of present or past psychiatric, neurological, or somatic disorders, or alcohol or drug-related problems. They took no medication at the time of the study. After thorough explanation of the study, written informed consent was obtained from all participants. The study was approved by the Regional Ethical Review Board in Stockholm, Sweden, and the Radiation Safety Committee at the Karolinska University Hospital Solna in Stockholm, Sweden.

PET procedures

[^{11}C]-L-deprenyl- D_2 was prepared by *N*-methylation of the desmethyl L-deprenyl- D_2 precursor using [^{11}C]methyl triflate as previously reported [9]. PET scans were carried out with the ECAT Exact HR 47 (Siemens/CTI, Knoxville, TN, USA), with an in-plane and an axial resolution of 3.6 and 4.0 mm at full width at half maximum (FWHM), respectively. A head fixation system with an individual plaster helmet was used. A 5-min transmission scan was performed using three rotating ^{68}Ge rod sources. Dynamic PET scan was performed for 63 min (10 s \times 9, 15 s \times 2, 20 s \times 3, 30 s \times 4, 1 min \times 4, 3 min \times 4, 6 min \times 7) after intravenous bolus injection of [^{11}C]-L-deprenyl- D_2 . Injected radioactivity was 299–520 MBq (419 ± 68 MBq), which were adjusted by body weight. Specific radioactivity was 104–341 GBq/ μmol (179 ± 80 GBq/ μmol) at the time of injection. Injected mass was 0.24–0.77 μg (0.50 ± 0.18 μg). Two PET scans were performed for each subject in the morning and in the afternoon on the same day.

Arterial blood sampling

Arterial blood was collected continuously for 10 min using an automated blood sampling system at a speed of 5 mL/min. Arterial blood was also drawn manually 1, 2, 4, 6, 8, 10, 15, 20, 30, 45, and 60 min after the injection for measurement of radioactivity in whole blood and plasma. The parent fraction of the radioligand was determined using a reversed-phase high-performance liquid chromatography (HPLC) method at 4, 10, 20, 30, 45, and 60 min. Plasma input function was defined as radioactivity of plasma multiplied by the percentage of unchanged radioligand.

Data analysis

PET images were reconstructed using the standard filtered back projection with a 2-mm Hanning filter, a zoom factor of 2.17, and a 128×128 matrix, and were corrected for attenuation and scatter. T1-weighted magnetic resonance imaging (MRI) was performed using a 1.5-T Siemens MAGNETOM Avanto for definition of anatomical brain regions and PVEc. The MR image was segmented into grey matter (GM), white matter (WM), and cerebrospinal fluid (CSF) segments, using the SPM5 segmentation algorithm in MATLAB (Wellcome Trust Centre for Neuroimaging, London, UK; The MathWorks, Inc., Natick, MA, USA). Regions of interest (ROI) were defined as the cerebellum, hippocampus, lateral frontal cortex, lateral occipital cortex, lateral parietal cortex, lateral temporal cortex, medial frontal cortex, putamen, and thalamus using the Anatomical Automatic Labeling (AAL) template [23]. GM masking was applied to the AAL template. All MRIs and ROIs were co-registered to summated PET images with the mutual information algorithm using SPM5. Regional radioactivity was calculated for each frame, corrected for decay, and plotted vs. time.

MAO-B binding of [^{11}C]-L-deprenyl- D_2 was quantified by two tissue compartment model (2TCM) with three rate constants (K_1 , k_2 , k_3) using metabolite-corrected plasma radioactivity as the input function. k_4 was set as 0 according to the assumption of irreversible binding of [^{11}C]-L-deprenyl- D_2 [7, 18]. Blood volume was fixed as 5%. The λk_3 defined as $(K_1/k_2) \times k_3$ was also calculated. These analyses were performed using the PMOD 3.4 software package (PMOD Group, Zurich, Switzerland).

PVEc

All PET data were corrected for PVE according to the method reported by Müller-Gärtner et al. [21]. In short, this PVEc corrects for spillover between GM and WM, and between GM and CSF using the segmented MR images. By assuming that the radioligand binding in WM is perfectly homogenous, every WM-voxel were replaced

by an average value derived from an isolated proportion of WM at the centrum semiovale [22].

Statistics

The test-retest variability of MAO-B binding as k_3 and λk_3 was expressed by the absolute difference between the first and second PET scans (PET1 and PET2) relative to the mean of the two values according to the following equation [24, 25]:

$$\%difference = \frac{|PET1 - PET2|}{((PET1 + PET2)/2)} \times 100$$

PET1 and PET2 are the parameters (k_3 or λk_3) of first and second PET scans, respectively.

Intraclass correlation coefficient (ICC) was also calculated by:

$$ICC = \frac{MSBS - MSWS}{MSBS + MSWS}$$

MSBS is the mean square of between subject, and MSWS is the mean square of within subject.

The correlation between MAO-B binding as k_3 or λk_3 and age was estimated using the Pearson correlation coefficient.

The effect of PVEc was estimates by the %change of before and after PVEc of all parameters, K_1 , k_2 , k_3 , and λk_3 :

$$\%change = \frac{\text{(after PVEc - before PVEc)}}{\text{before PVEc}} \times 100$$

In both analysis of age effect and PVEc, average values of PET1 and PET2 were used. Finally, the test-retest variability of after PVEc was estimated as same way as before PVEc.

These statistical analyses were performed using R 3.3.2 (The R Foundation, Vienna, Austria).

Results

Test-retest variability

Mean and SD values of six subjects in PET1 and PET2, mean and range of %differences, and ICC in all regions are shown in Table 1. %difference of k_3 was 2.6% (medial frontal cortex) to 10.3% (hippocampus), and that of λk_3 was 5.0% (thalamus) to 9.2% (cerebellum). Mean %difference of nine regions were 5.3% and 7.0% in k_3 and λk_3 , respectively. All regions showed variability below 10%, except the hippocampus in k_3 (10.3%). ICC of k_3 was 0.78 (hippocampus) to 0.98 (medial frontal cortex), and that of λk_3 was 0.78 (hippocampus) to 0.95 (thalamus). Mean ICC of nine regions were 0.94 and 0.89 in k_3 and λk_3 , respectively.

Age effect

The Pearson correlation coefficient and p value between k_3 or λk_3 and age in all regions are shown in Table 2. The highest positive correlation was observed in the hippocampus ($r = 0.75$ in k_3 and 0.76 in λk_3 ; Fig. 1a, b). Regardless, both results were not statistically significant ($p = 0.08$ and $p = 0.08$, respectively).

PVEc

After PVEc, K_1 values increased as 36.9 to 62.7% according to the age (Fig. 2). %change of λk_3 was 23.5 to 37.0% and also correlated with age. Compared to K_1 and λk_3 , k_2 and k_3 showed only small changes after PVEc (11.6 to 15.4% and -1.3 to 5.5%, respectively).

Mean and SD values of six subjects in PET1 and PET2, mean and range of %differences, and ICC after PVEc in all regions are shown in Table 3. Mean %difference of nine regions were 5.6 and 7.2% in k_3 and λk_3 , respectively. Mean ICC of nine regions were 0.92 and 0.90 in k_3 and λk_3 , respectively. These values were almost the same as those before PVEc.

Table 1 Mean and SD values in PET1 and PET2, mean and range of %differences, and ICC in all regions of k_3 and λk_3

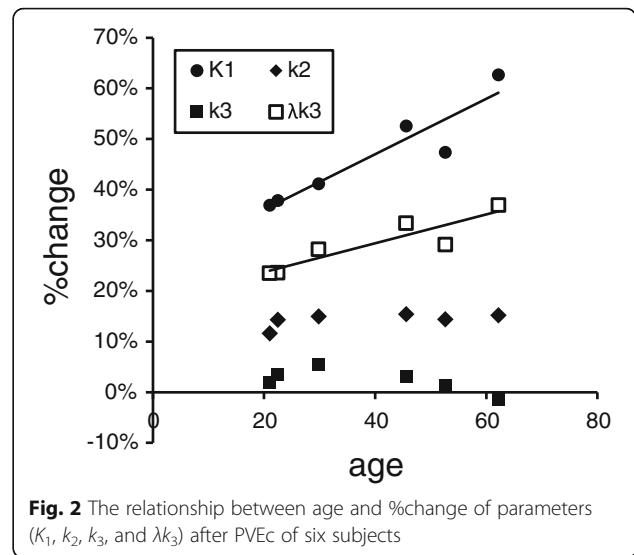
Region	k_3			λk_3										
	PET1		PET2		%dif		PET1		PET2		%dif			
	Mean	SD	Mean	SD	Mean	Range	ICC	Mean	SD	Mean	SD	Mean	Range	ICC
Cerebellum	0.051	0.011	0.051	0.012	5.1	0.7–11.1	0.96	0.143	0.030	0.140	0.031	9.2	5.9–15.4	0.90
Hippocampus	0.103	0.023	0.108	0.017	10.3	0.2–20.6	0.78	0.288	0.028	0.285	0.047	6.4	1.0–17.6	0.78
Lateral frontal cortex	0.067	0.014	0.067	0.013	3.8	0.4–7.2	0.97	0.185	0.023	0.184	0.033	6.0	2.4–14.2	0.91
Lateral occipital cortex	0.060	0.013	0.061	0.013	6.4	1.0–15.1	0.92	0.175	0.024	0.170	0.030	8.0	3.0–15.0	0.86
Lateral parietal cortex	0.063	0.012	0.064	0.012	3.7	1.4–7.7	0.97	0.180	0.027	0.182	0.035	7.2	2.5–12.1	0.91
Lateral temporal cortex	0.065	0.015	0.063	0.015	5.9	0.1–13.7	0.95	0.201	0.029	0.199	0.041	8.3	2.2–20.0	0.86
Medial frontal cortex	0.068	0.012	0.067	0.011	2.6	1.1–4.6	0.98	0.175	0.019	0.175	0.026	5.7	2.8–10.1	0.89
Putamen	0.087	0.019	0.085	0.016	5.4	3.2–7.6	0.96	0.323	0.051	0.331	0.072	7.4	3.0–10.5	0.91
Thalamus	0.083	0.017	0.082	0.017	4.2	0.1–9.4	0.97	0.306	0.047	0.308	0.059	5.0	1.5–8.6	0.95

Table 2 The Pearson correlation coefficient and p value between age and parameters in all regions of k_3 and λk_3

Region	k_3		λk_3	
	r	p	r	p
Cerebellum	0.58	0.23	0.56	0.25
Hippocampus	0.75	0.08	0.76	0.08
Lateral frontal cortex	0.65	0.17	0.73	0.10
Lateral occipital cortex	0.66	0.16	0.59	0.22
Lateral parietal cortex	0.70	0.13	0.64	0.18
Lateral temporal cortex	0.69	0.13	0.72	0.10
Medial frontal cortex	0.58	0.22	0.66	0.15
Putamen	0.67	0.15	0.75	0.09
Thalamus	0.69	0.13	0.63	0.18

Discussion

In this study, the test-retest variability of [^{11}C]-L-deprenyl- D_2 was estimated using healthy subjects. Mean of absolute %difference in nine regions of λk_3 was 7.0%, indicating good reproducibility. The test-retest variability of λk_3 using %difference (not absolute difference) by Logan et al. was previously reported as $-2.84 \pm 7.07\%$ [18]. The same calculation of our data yielded $-1.1 \pm 8.3\%$, indicating similar variability. ICC values were high in all regions, except in the hippocampus which was relatively low (0.78). It also indicated good reproducibility of [^{11}C]-L-deprenyl- D_2 . Our research group recently reported the brain occupancy of MAO-B using [^{11}C]-L-deprenyl- D_2 after administration of a MAO-B inhibitor—sebragiline [9]. The study reported that oral administrations of 1–5 mg sebragiline induced near-maximal inhibition of brain MAO-B, and MAO-B occupancy was correlated with the plasma concentration of sebragiline in patients with AD. The good test-retest reproducibility of the present study using same procedure of [^{11}C]-L-deprenyl- D_2 preparation and same PET camera corroborates the findings of our previous study.



Although λk_3 is generally considered to be a more stable outcome measure than k_3 [7, 18], k_3 showed similar %difference as λk_3 (5.3 vs 7.0%) in the present study. k_3 values also showed better ICC than those of λk_3 (mean value, 0.94 vs 0.89). These findings indicate that k_3 may be independently used for further studies such as comparison between patients and healthy controls or target occupancy of MAO-B inhibitors. Obvious regional differences of reproducibility were only observed in the hippocampus. The reason of low reproducibility in the hippocampus is not clear, but one possibility is that its high k_3 value (the highest among all regions) may have induced a large variability.

In this study, two PET measurements were performed in 1 day, in the morning and afternoon. Several studies suggested that dopamine system was affected by the circadian rhythm [26–28]. Especially, one rodent study reported that MAO-A expression was regulated by the clock-component gene [29]. However, our result did not show the relation between the MAO-B binding and the time of PET measurements.

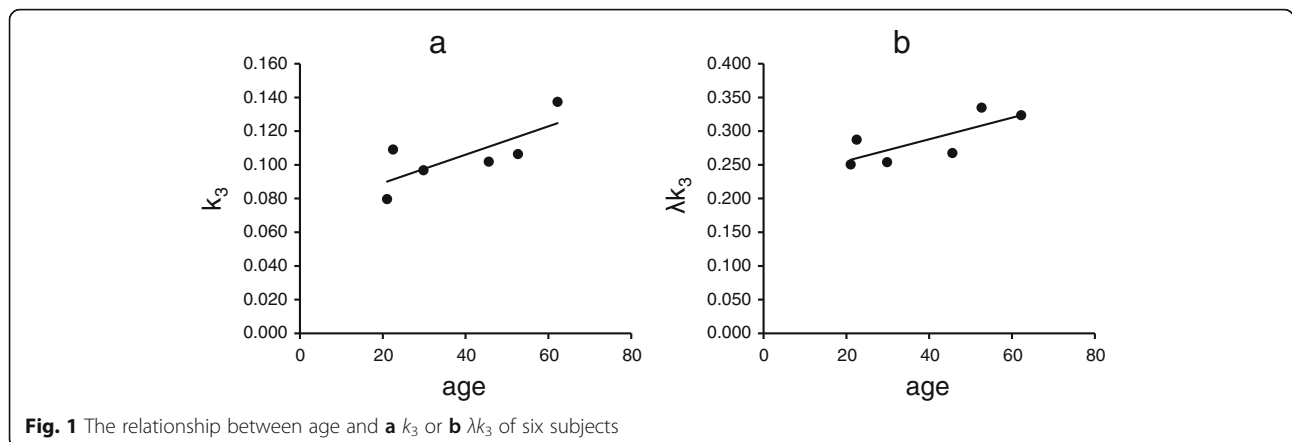


Table 3 Mean and SD values in PET1 and PET2, mean and range of %differences, and ICC in all regions of k_3 and λk_3 after PVEc

Region	k_3							λk_3						
	PET1		PET2		%dif			PET1		PET2		%dif		
	Mean	SD	Mean	SD	Mean	Range	ICC	Mean	SD	Mean	SD	Mean	Range	ICC
Cerebellum	0.050	0.011	0.051	0.012	5.6	1.1–11.2	0.95	0.174	0.039	0.170	0.040	9.8	5.6–16.1	0.91
Hippocampus	0.116	0.024	0.122	0.019	10.6	0.3–23.2	0.70	0.345	0.028	0.340	0.055	7.4	1.4–17.7	0.73
Lateral frontal cortex	0.065	0.012	0.065	0.012	4.0	1.5–7.1	0.97	0.272	0.050	0.271	0.063	6.2	2.0–15.0	0.95
Lateral occipital cortex	0.059	0.010	0.059	0.012	7.2	1.4–16.7	0.86	0.243	0.039	0.233	0.047	9.1	1.3–19.8	0.84
Lateral parietal cortex	0.062	0.011	0.064	0.011	4.0	1.3–7.2	0.96	0.265	0.049	0.267	0.059	7.7	2.9–12.3	0.93
Lateral temporal cortex	0.065	0.014	0.063	0.014	6.0	0.4–14.4	0.95	0.264	0.046	0.260	0.061	9.0	2.1–22.8	0.88
Medial frontal cortex	0.065	0.010	0.065	0.010	2.2	0.5–4.2	0.98	0.265	0.041	0.267	0.052	5.1	0.0–9.1	0.94
Putamen	0.089	0.018	0.086	0.017	4.8	1.1–7.6	0.96	0.329	0.053	0.337	0.076	7.0	0.4–12.0	0.91
Thalamus	0.095	0.020	0.096	0.018	6.3	1.7–10.5	0.92	0.326	0.061	0.325	0.072	3.9	0.0–8.5	0.96

A moderate age effect on λk_3 values was observed in all regions. The degree of increase (6.3% per decade) was similar as the previously reported value by Fowler et al., at 7.1% per decade [20]. One postmortem study also reported increasing of MAO-B protein in the human brain according to age [19]. Our PET study confirmed both findings of postmortem and in vivo human brain studies. Among all regions, the hippocampus showed the highest correlation with age effect although it did not reach statistical significance and the reproducibility was relatively low as discussed above. Since the hippocampus is thought to be especially impacted in AD [30, 31], the present findings suggest the increase of MAO-B activity may have an important role about the pathology of AD.

PVE should be considered in PET studies when brain atrophy is observed in aged subjects or patients with disorders such as AD. Additionally, PVE is larger using a low resolution PET camera than a high resolution one. This study included elderly subjects and was conducted using relatively low resolution PET camera system compared to recent PET systems like the high resolution research tomograph (HRRT) with 1.5 mm FWHM [32]. In the present study, %change of K_1 after PVEc was correlated with age. It indicates that the brain of aged subjects was more affected by the PVE compared to younger subject due to the brain atrophy. Meanwhile, k_2 and k_3 did not show any clear change after PVEc. λk_3 was also moderately affected by PVEc and correlated with age since it is partially determined by K_1/k_2 . Nevertheless, although the value itself of λk_3 was increased in aged subjects, test-retest variability of λk_3 did not change after PVEc. This indicates that PVEc can reliably keep reproducibility even in the case of elderly subjects with brain atrophy.

There are several imitations in this study. Although only six subjects were included and it is relatively small sample size, the number were similar as previous

test-retest studies about [^{11}C]-L-deprenyl- D_2 by Logan et al. ($n = 5$) [18] and other PET radioligands ($n = 6-8$) [25, 33]. However, the studies about age effect included larger number generally [20, 34, 35]. So, the present result about the age effect might be preliminary. Additionally, only healthy control subjects were included in this study. It is difficult to extrapolate our findings about PVEc to AD patients because the elderly ones showed slight atrophy but not pathological. To more accurately estimate the effects of PVEc, further studies with AD patients and aged control subjects who showed strong atrophy will be needed.

Conclusions

The present results indicate that k_3 and λk_3 of [^{11}C]-L-deprenyl- D_2 are reliable parameters for test-retest reproducibility with healthy subjects both before and after PVEc. As the number of subjects was relatively small and only healthy subjects were included, the studies with patients of larger sample size are required for further clinical applications.

Abbreviations

2TCM: Two tissue compartment model; AAL: Anatomical Automatic Labeling; AD: Alzheimer's disease; ALS: Amyotrophic lateral sclerosis; CSF: Cerebrospinal fluid; FWHM: Full width at half maximum; GM: Grey matter; HRRT: High resolution research tomograph; ICC: Intraclass correlation coefficient; MAO: Monoamine oxidase; MRI: Magnetic resonance image; MSBS: Mean square of between subject; MSWS: Mean square of within subject; PET: Positron emission tomography; PVE: Partial volume effect; PVEc: Partial volume effect correction; ROI: Regions of interest; WM: White matter

Acknowledgements

We thank all members of the Karolinska Institutet PET Centre for assistance with the PET experiments. RSM was recipient of a post doc fellowship (CNPq-23364/2014-7).

Funding

This work was partially supported by GE Healthcare Ltd., UK.

Authors' contributions

PS, AT, and CH designed the study and wrote the protocol. PS and SN conducted the PET experiment. RA, PS, AT, and RSM analyzed the data. RA wrote the first draft of the manuscript. All authors read and approved the final manuscript.

Competing interests

The authors declare that they have no competing interests.

Consent for publication

Not applicable

Ethics approval and consent to participate

The study was approved by the Regional Ethical Review Board in Stockholm, Sweden, and the Radiation Safety Committee at the Karolinska University Hospital in Solna in Stockholm, Sweden. After thorough explanation of the study, written informed consent was obtained from all participants.

Publisher's Note

Springer Nature remains neutral with regard to jurisdictional claims in published maps and institutional affiliations.

Author details

¹Department of Clinical Neuroscience, Center for Psychiatry Research, Karolinska Institutet and Stockholm County Council, Stockholm, Sweden. ²Primate Center and Laboratory of Neurosciences and Behavior, Department of Physiological Sciences, Institute of Biology, University of Brasilia, Brasilia, Brazil.

Received: 24 April 2017 Accepted: 9 June 2017

Published online: 20 June 2017

References

- Finberg JPM. Update on the pharmacology of selective inhibitors of MAO-A and MAO-B: focus on modulation of CNS monoamine neurotransmitter release. *Pharmacol Ther.* 2014;143:133–52.
- Gulyás B, Pavlova E, Kása P, Gulya K, Bakota L, Várszegi S, et al. Activated MAO-B in the brain of Alzheimer patients, demonstrated by [¹¹C]-deprenyl using whole hemisphere autoradiography. *Neurochem Int.* 2011;58:60–8.
- Emilsson L, Saetre P, Balciniene J, Castensson A, Cairns N, Jazin EE. Increased monoamine oxidase messenger RNA expression levels in frontal cortex of Alzheimer's disease patients. *Neurosci Lett.* 2002;326:56–60.
- Saura J, Luque JM, Cesura AM, Da Prada M, Chan-Palay V, Huber G, et al. Increased monoamine oxidase B activity in plaque-associated astrocytes of Alzheimer brains revealed by quantitative enzyme radioautography. *Neuroscience.* 1994;62:15–30.
- Jossan SS, Gillberg PG, Gottfries CG, Karlsson I, Oreland L. Monoamine oxidase B in brains from patients with Alzheimer's disease: a biochemical and autoradiographical study. *Neuroscience.* 1991;45:1–12.
- Nakamura S, Kawamata T, Akiguchi I, Kameyama M, Nakamura N, Kimura H. Expression of monoamine oxidase B activity in astrocytes of senile plaques. *Acta Neuropathol.* 1990;80:419–25.
- Fowler JS, Wang GJ, Logan J, Xie S, Volkow ND, MacGregor RR, et al. Selective reduction of radiotracer trapping by deuterium substitution: comparison of carbon-11-L-deprenyl and carbon-11-deprenyl-D2 for MAO B mapping. *J Nucl Med.* 1995;36:1255–62.
- Hirvonen J, Kailajärvi M, Haltia T, Koskimies S, Nägren K, Virsu P, et al. Assessment of MAO-B occupancy in the brain with PET and [¹¹C]-deprenyl-D2: a dose-finding study with a novel MAO-B inhibitor, EVT 301. *Clin Pharmacol Ther.* 2009;85:506–12.
- Sturm S, Forsberg A, Nave S, Stenkrona P, Seneca N, Varrone A, et al. Positron emission tomography measurement of brain MAO-B inhibition in patients with Alzheimer's disease and elderly controls after oral administration of sebragiline. *Eur J Nucl Med Mol Imaging.* 2017;44(3):382–91.
- Carter SF, Schöll M, Almkvist O, Wall A, Engler H, Långström B, et al. Evidence for astrocytosis in prodromal Alzheimer disease provided by ¹¹C-deuterium-L-deprenyl: a multitracers PET paradigm combining ¹¹C-Pittsburgh compound B and ¹⁸F-FDG. *J Nucl Med.* 2012;53:37–46.
- Choo ILH, Carter SF, Schöll ML, Nordberg A. Astrocytosis measured by ¹¹C-deprenyl PET correlates with decrease in gray matter density in the parahippocampus of prodromal Alzheimer's patients. *Eur J Nucl Med Mol Imaging.* 2014;41:2120–6.
- Santillo AF, Gambini JP, Lannfelt L, Långström B, Ulla-Marja L, Kilander L, et al. In vivo imaging of astrocytosis in Alzheimer's disease: an ¹¹C-L-deuteriodeprenyl and PIB PET study. *Eur J Nucl Med Mol Imaging.* 2011;38:2202–8.
- Johansson A, Engler H, Blomquist G, Scott B, Wall A, Aquilonius S-M, et al. Evidence for astrocytosis in ALS demonstrated by [¹¹C](L)-deprenyl-D2 PET. *J Nucl Med.* 2007;255:17–22.
- Fowler JS, Volkow ND, Cileto R, Wang GJ, Felder C, Logan J. Comparison of brain glucose metabolism and monoamine oxidase B (MAO B) in traumatic brain injury. *Clin Positron Imaging.* 1999;2:71–9.
- Bergström M, Kumlien E, Lilja A, Tyrefors N, Westerberg G, Långström B. Temporal lobe epilepsy visualized with PET with ¹¹C-L-deuterium-deprenyl—analysis of kinetic data. *Acta Neurol Scand.* 1998;98:224–31.
- Kumlien E, Bergström M, Lilja A, Andersson J, Szekeres V, Westerberg CE, et al. Positron emission tomography with [¹¹C]deuterium-deprenyl in temporal lobe epilepsy. *Epilepsia.* 1995;36:712–21.
- Kumlien E, Nilsson A, Hagberg G, Långström B, Bergström M. PET with ¹¹C-deuterium-deprenyl and ¹⁸F-FDG in focal epilepsy. *Acta Neurol Scand.* 2001;103:360–6.
- Logan J, Fowler JS, Volkow ND, Wang GJ, MacGregor RR, Shea C. Reproducibility of repeated measures of deuterium substituted [¹¹C]-deprenyl ([¹¹C]-deprenyl-D2) binding in the human brain. *Nucl Med Biol.* 2000;27:43–9.
- Tong J, Meyer JH, Furukawa Y, Boileau I, Chang L-J, Wilson AA, et al. Distribution of monoamine oxidase proteins in human brain: implications for brain imaging studies. *J Cereb Blood Flow Metab.* 2013;33:863–71.
- Fowler JS, Volkow ND, Wang GJ, Logan J, Pappas N, Shea C, et al. Age-related increases in brain monoamine oxidase B in living healthy human subjects. *Neurobiol Aging.* 1997;18:431–5.
- Müller-Gärtner HW, Links JM, Prince JL, Bryan RN, McVeigh E, Leal JP, et al. Measurement of radiotracer concentration in brain gray matter using positron emission tomography: MRI-based correction for partial volume effects. *J Cereb Blood Flow Metab.* 1992;12:571–83.
- Schain M, Tóth M, Cselényi Z, Stenkrona P, Halldin C, Farde L, et al. Quantification of serotonin transporter availability with [¹¹C]MADAM—a comparison between the ECAT HRRT and HR systems. *Neuroimage.* 2012;60:800–7.
- Tzourio-Mazoyer N, Landeau B, Papathanassiou D, Crivello F, Etard O, Delcroix N, et al. Automated anatomical labeling of activations in SPM using a macroscopic anatomical parcellation of the MNI MRI single-subject brain. *Neuroimage.* 2002;15:273–89.
- Collste K, Forsberg A, Varrone A, Amini N, Ainehband S, Yakushev I, et al. Test–retest reproducibility of [¹¹C]PBR28 binding to TSPO in healthy control subjects. *Eur J Nucl Med Mol Imaging.* 2016;43:173–83.
- Nord M, Finnema SJ, Schain M, Halldin C, Farde L. Test–retest reliability of [¹¹C]AZ10419369 binding to 5-HT1B receptors in human brain. *Eur J Nucl Med Mol Imaging.* 2014;41:301–7.
- Cervenka S, Halldin C, Farde L. Age-related diurnal effect on D2 receptor binding: a preliminary PET study. *Int J Neuropsychopharmacol.* 2008;11:671–8.
- Minton GO, Young AH, McQuade R, Fairchild G, Ingram CD, Gartside SE. Profound changes in dopaminergic neurotransmission in the prefrontal cortex in response to flattening of the diurnal glucocorticoid rhythm: implications for bipolar disorder. *Neuropsychopharmacology.* 2009;34:2265–74.
- Huang J, Zhong Z, Wang M, Chen X, Tan Y, Zhang S, et al. Circadian modulation of dopamine levels and dopaminergic neuron development contributes to attention deficiency and hyperactive behavior. *J Neurosci.* 2015;35:2572–87.
- Hampp G, Ripberger JA, Houben T, Schmutz I, Blex C, Perreau-Lenz S, et al. Regulation of monoamine oxidase A by circadian-clock components implies clock influence on mood. *Curr Biol.* 2008;18:678–83.
- Braskie MN, Thompson PM. A focus on structural brain imaging in the Alzheimer's disease neuroimaging initiative. *Biol Psychiatry.* 2014;75:527–33.
- de Flores R, La Joie R, Chételat G. Structural imaging of hippocampal subfields in healthy aging and Alzheimer's disease. *Neuroscience.* 2015;309:29–50.
- Varrone A, Sjöholm N, Eriksson L, Gulyás B, Halldin C, Farde L. Advancement in PET quantification using 3D-OP-OSEM point spread function reconstruction with the HRRT. *Eur J Nucl Med Mol Imaging.* 2009;36:1639–50.

33. Jučaitė A, Cselényi Z, Arvidsson A, Ahlberg G, Julin P, Varnäs K, et al. Kinetic analysis and test-retest variability of the radioligand [11C](R)-PK11195 binding to TSPO in the human brain—a PET study in control subjects. *EJNMMI Res.* 2012;2:15.
34. Fazio P, Schain M, Mrzljak L, Amini N, Nag S, Al-Tawil N, et al. Patterns of age related changes for phosphodiesterase type-10A in comparison with dopamine D 2/3 receptors and sub-cortical volumes in the human basal ganglia: a PET study with 18 F-MNI-659 and 11 C-raclopride with correction for partial volume effect. *Neuroimage.* 2017;152:330–9.
35. Matuskey D, Worhunksy P, Correa E, Pittman B, Gallezot J-D, Nabulsi N, et al. Age-related changes in binding of the D2/3 receptor radioligand [11C](+)-PHNO in healthy volunteers. *Neuroimage.* 2016;130:241–7.

Submit your manuscript to a SpringerOpen[®] journal and benefit from:

- ▶ Convenient online submission
- ▶ Rigorous peer review
- ▶ Open access: articles freely available online
- ▶ High visibility within the field
- ▶ Retaining the copyright to your article

Submit your next manuscript at ▶ springeropen.com
